This is the accepted manuscript made available via CHORUS. The article has been published as:

Ab initio finite-temperature elasto-optic response in ferroelectrics: The case of math xmlns="http://www.w3.org/1998/Math/MathML">msub>mi>BaTiO/mi>mn>3/mn>/msub>/math> and math xmlns="http://www.w3.org/1998/Math/MathML">mrow>msub>mi>Ba/mi>mrow>mn>1/mn>mo>−/mo>mi>x/mi>/mrow>/msub>msub>mi>Sr/mi>mi>x/mi>/msub>msub>mi>TiO/mi>mn>3/mn>/msub>/mrow>/math>

Sergey Prosandeev, Charles Paillard, and L. Bellaiche

Phys. Rev. B **110**, L220102 — Published 26 December 2024

DOI: 10.1103/PhysRevB.110.L220102

Ab-initio finite temperature elasto-optic response in ferroelectrics: the case of $BaTiO_3$ and $Ba_{1-x}Sr_xTiO_3$

Sergey Prosandeev,[1,*] Charles Paillard,[1,2,†] and L. Bellaiche[1,3,‡]

[1]*Smart Ferroic Materials Center, Department of Physics and Institute for Nanoscience and Engineering, University of Arkansas, Fayetteville, Arkansas 72701, USA*

[2]*Université Paris-Saclay, CentraleSupélec, CNRS, Laboratoire SPMS, 91190, Gif-sur-Yvette, France.*

[3]*Department of Materials Science and Engineering, Tel Aviv University, Ramat Aviv, Tel Aviv 6997801, Israel.*

Abstract

Elasto-optic effects characterize the dependency of optical birefringence on strain. Thus, by changing the strain, one can control the optical properties of the sample. Large elasto-optic effects are desirable to improve the sensitivity of elasto-optic devices, their performances and lower their energy consumption. Yet, the microscopic mechanisms underlying elasto-optic conversion effects are not well understood. For example, the temperature dependencies of the elasto-optic effect as well as the effect of the concentration in solid solutions have not been investigated from first principles. Here, we develop a coupled Density Functional Theory and effective Hamiltonian numerical method to compute and understand the elasto-optic response of ferroelectric materials at finite temperature. In particular, we apply such scheme to calculate the elasto-optic response of $BaTiO_3$ and $Ba_{1-x}Sr_xTiO_3$ compounds in their tetragonal phase near room temperature, and report how elasto-optic coefficients can be significantly enhanced in the visible range. We also demonstrate that, and explain why, this effect can be enlarged in the THz frequency range.

The elasto-optic effect, in which a mechanical strain modifies the optical index, is critical to many technologies such as optical filters [1], acousto-optic modulators for photonics [2] or optical strain gauges [3]. The performance of these devices critically depends on the magnitude of the elasto-optic constants. Indeed, large elasto-optic constants are required for these devices to work efficiently. Investigations and strategies on how to control elasto-optic conversion are therefore presently needed. At the same time, experimental studies of this effect are currently rather limited, most likely because of the complexity of the measurement of the elasto-optic constants. For example, for the model ferroelectric system, that is $BaTiO_3$ (BTO), these data are only known at room temperature. The possibility to enhance the elasto-optic effect in BTO-based solid solutions has also not been intensively explored, to the best of our knowledge. Consequently, predicting and understanding ways of controlling elasto-optic conversion is a current critical challenge.

The advent of *ab initio* tools relying on Density Functional Theory (DFT) to predict, with a certain degree of accuracy, the optical properties of materials, offers new opportunities to discover and understand novel elasto-optic or electro-optic materials [4]. Unfortunately, DFT usually predicts electro- or elasto-optic properties at 0 K. In many cases, this is acceptable as

* sprossan@uark.edu

† paillard@uark.edu

‡ laurent@uark.edu

demonstrated in the case of $LiNbO_3$ [5]. However, in $BaTiO_3$ (BTO), exhibiting a tetragonal ferroelectric phase at room temperature which is otherwise unstable at 0 K, predicting the electro- and elasto-optic response from DFT *ab initio* becomes a daunting task which has likely impeded the discovery of novel and more efficient electro- or elasto-optic materials. In fact, in BTO, studies have been limited to the low-temperature rhombohedral phase which is not observed at room temperature [6]. Therefore, the problem of understanding the room-temperature elasto-optic effect in perovskites such as BTO has mostly relied on analytical theories [7, 8] which, e.g., do not consider ionic effects on the elasto-optic response. These latter may be important, for instance, in the THz regime as our recent work on the electro-optic response of BTO highlighted [9]. Similarly, previous uses of DFT to calculate the elasto-optic response from varying the strain of unit cells and calculating the optical dielectric response [10–13] do not account either for the important ionic dynamical response that may occur in the THz regime and below.

Recently, and based upon earlier works from Veithen *et al.* [14], we proposed a coupled DFT and effective Hamiltonian numerical scheme able to calculate the electro-optic response of materials at finite temperatures [9], while also being able to deal with a broader range of electromagnetic radiation, from the visible to the THz regime and below. Yet, no such methodology exists for the *elasto-optic* response, that is, until now. This is all the more important since elasto-optic responses are ubiquitous in all materials (in stark contrast with linear electro-optic effects which are limited to non-centrosymmetric materials), and thus offer a much broader playground to develop control of the optical index.

We address this important problem in this Letter. First, we develop the formalism describing the finite-temperature elasto-optic response and implement it numerically by combining DFT and effective Hamiltonian-based methods on the specific cases of BTO and $Ba_{1-x}Sr_xTiO_3$ (BST) solid solutions. Our predictions agree reasonably well with the currently available experimental data (that only exist at room temperature [15]. Then we proceed to reveal that some elasto-optic responses, in the visible part of the electromagnetic spectrum, of BTO (and BST) are significantly enhanced at temperatures (compositions, respectively) close to the tetragonal polar to cubic paraelectric phase transition, as was for instance already observed and explained in the cubic phase of $BaTiO_3$ [7]. Other elasto-optic coefficients rather adopt a minimum near this transition or are nearly insensitive to temperature. We also reveal (1) the microscopic origin of such different behaviors, and (2)

the drastically different origin of the elasto-optic response in the THz regime (with respect to the visible range), where a strong ionic contribution dominates over the elasto-optic response of valence electrons.

We start by deriving the formalism which will allow to compute the finite-temperature elasto-optic response by analogy with previous works on the finite-temperature electro-optic response [9, 14]. The formula defining the elasto-optic coefficients at constant electric field, $p^E_{ij\alpha\beta}$ [15], is:

$$p^E_{ij\alpha\beta}(\omega,\nu) = \frac{d(\frac{1}{\varepsilon_{ij}(\omega)})}{d\eta_{\alpha\beta}(\nu)} \tag{1}$$

where $\varepsilon_{ij}(\omega)$ is the total dielectric constant at frequency ω and $\eta_{\alpha\beta}(\nu)$ are the elements of the homogeneous strain tensor at frequency ν.

$\varepsilon_{ij}(\omega)$ can be separated into a purely electronic part, $\varepsilon^{el}_{ij}(\omega)$, associated with the electronic polarization, and the ionic dielectric susceptibility associated with the ionic polarization $\chi^{ion}_{ij}(\omega)$:

$$\varepsilon_{ij}(\omega) = \varepsilon^{el}_{ij}(\omega) + \chi^{ion}_{ij}(\omega) \tag{2}$$

Consequently, the elasto-optic coefficients can be decomposed into an electronic component, $p^{E,el}_{ij\alpha\beta}(\omega,\nu)$, and an ionic part, $p^{E,ion}_{ij\alpha\beta}(\omega,\nu)$:

$$p^E_{ij\alpha\beta}(\omega,\nu) = p^{E,el}_{ij\alpha\beta}(\omega,\nu) + p^{E,ion}_{ij\alpha\beta}(\omega,\nu) \tag{3}$$

with:

$$p^{E,el}_{ij\alpha\beta}(\omega,\nu) = -\frac{1}{\varepsilon_{ii}(\omega)\varepsilon_{jj}(\omega)}\left[\left(\frac{\partial\varepsilon^{el}_{ij}(\omega)}{\partial\eta_{\alpha\beta}(\nu)}\right)_{\mathbf{P}} + \sum_\gamma \left(\frac{\partial\varepsilon^{el}_{ij}(\omega)}{\partial P_\gamma(\nu)}\right)_{\boldsymbol{\eta}} \frac{dP_\gamma(\nu,T)}{d\eta_{\alpha\beta}(\nu)}\right]. \tag{4}$$

$P_\gamma(\nu)$ is the γ-th Cartesian component of the polarization ($\gamma = 1, 2,$ or 3, corresponding to the [100], [010] and [001] pseudo-cubic axes, respectively) at frequency ν.

The ionic contribution to the elasto-optic response takes the form:

$$p^{E,ion}_{ij\alpha\beta}(\nu,\omega) = -\frac{1}{\varepsilon_{ii}(\omega)\varepsilon_{jj}(\omega)}\frac{d\chi^{ion}_{ij}(\omega,T)}{d\eta_{\alpha\beta}(\nu)} \tag{5}$$

One must remember that $\varepsilon_{ii}(\omega)$ and $\varepsilon_{jj}(\omega)$ appearing in Eqs. (4-5) involve both the electronic and ionic dielectric responses. Let us also emphasize that Eqs. (1&5) involve *full* derivatives with respect to strains. In contrast, partial derivatives with respect to strain (at constant polarization) and polarization (at constant strain) appear in the right-hand

side of Eq. (4) – in addition to the full derivative of the γ-th Cartesian component of the polarization with respect to $\eta_{\alpha\beta}(\nu)$. Typically, for ω belonging to frequencies in the *optical range*, the ionic part provided by Eq. (5) is much smaller than the electronic contribution of Eq. (4), as done in Ref. [14]. On the other hand, at *THz and lower frequencies*, the ionic contribution should be included as demonstrated in Ref. [9]. Lastly, we consider only low-frequency strain excitations ν, and thus practically consider $\nu = 0$.

Based on Eqs. (4-5), we can now compute the finite-temperature elasto-optic coefficients. We will, in the following, consider the model ferroelectric system BTO and solid solutions BST, which both exhibit a ferroelectric $P4mm$ phase at room temperature at low x. The elasto-optic tensor, in the $P4mm$ space group, has seven independent components: p^E_{1111}, p^E_{1122}, p^E_{1133}, p^E_{3311}, p^E_{3333}, p^E_{1313} and p^E_{1212}, whose expression is detailed in the Supplemental Material [16–22].

According to the measurements of Ref. [15] (which states that they determine "absolute values" for most elasto-optic coefficients), $\left|p^E_{3333}\right| = 0.77$ and $\left|p^E_{1133}\right| = 0.20$ are significant elasto-optic responses in the tetragonal phase of BTO. These latter involve the applications of longitudinal strain η_{33} along the polar axis (see Eq. (1) of the SM [16]). Similarly, according to experiment [15], $\left|p^E_{1313}\right| = 1.0$ at room temperature is a large elasto-optic coefficient in BTO. It involves the optical response to the applied shear strain η_{13} [16]. In order to demonstrate different temperature behaviors (to be discussed later on), we will also consider the p^E_{1122} and p^E_{1212} elastooptic coefficients. Interestingly, p^E_{1122} involves the derivative of the component of the polarization along the polar axis but with respect to the in-plane η_{22} strain while p^E_{1212} does not depend on derivatives of the polarization components with respect to strains [16]. We thus focus primarily on the coefficients p^E_{1122}, p^E_{1133}, p^E_{3333}, p^E_{1313} and p^E_{1212}.

To calculate the electronic dielectric constant and its derivatives involved in Eq. (4), we employ the Abinit DFT package [23]. The Local Density Approximation is used with optimized norm-conserving Vanderbilt pseudopotentials ONCVPSP-3.2.3 [24]. BST solid solutions are treated using the virtual crystal alloy approximation [25]. The electronic dielectric constant at frequency ω is calculated in the Independent Particle Approximation (IPA) [26]. Its relevant derivatives with respect to polarization and strains, appearing in Eq. (4), are calculated using a central finite difference scheme with second order accuracy [16] by separately varying the soft mode amplitude by ± 10 % and the relevant strain components by ± 0.05. Finite temperature effects are effectively recovered from the full derivatives of the

polarization components with respect to strain, $\frac{dP_\gamma}{d\eta_{\alpha\beta}}$, appearing in Eq. 4. These terms are strongly dependent on temperature, because they are related to the ferroelectric soft mode. We computed them at selected finite temperatures, with the help of Monte-Carlo simulations based on the Effective Hamiltonian method of BST (that remains valid for BTO) described in Ref. [22]. Technical details are further described in the Supplemental Material [16].

We anticipate, as revealed in Ref. [9] for the electro-optic effects, that for ω in the THz range or below, the ionic response in Eq. (5) may become significant. In such cases, in addition to the electronic terms from Eq. (4) calculated at frequency ω (see the previous paragraphs), we must calculate both $\chi_{ii}^{ion}(\omega)$ which contributes to the total dielectric permittivity $\varepsilon_{ii}(\omega)$ involved in Eqs (4) and (5) and the derivatives of the ionic dielectric susceptibility $\frac{d\chi_{ij}^{ion}(\omega)}{d\eta_{\alpha\beta}}$. Technically, this last term can be computed from the finite differences of the effective Hamiltonian-based finite temperature Molecular Dynamics (MD) simulation's calculations of $\chi_{ij}^{ion}(\omega)$ performed at different strains. Such calculation requires a high precision on the dielectric susceptibility and its derivatives with respect to the strain. However, the real part of the ionic dielectric permittivity in ferroelectrics can have rather large values and, near the resonance, it can change significantly, both in magnitude and sign. The position of the resonance strongly depends on the ferroelectric mode. In the tetragonal phase of BTO, the T_{1u} ferroelectric mode of the cubic paraelectric phase splits into E and A modes. The A mode corresponds to the shift of the atoms along the polarization. This mode, below the phase transition point, rapidly becomes hard and our effective Hamiltonian indicates that its typical frequency is of about 10 THz at 300 K [27], in good agreement with the Slater-type A-mode frequency measured around 250 - 275 cm^{-1} (8 THz) [28]. Therefore we expect the ionic dielectric susceptibility components such as χ_{33}^{ion} and its derivatives to be fairly constant far below from the resonance of the A-mode (*i.e.,* well below 9 THz) and vanishingly small well above. Practically, we found the real part of χ_{33}^{ion} to be negligible above 18 THz. We will thus focus, in the following, on two limiting cases: (1) the visible or near-Infrared electromagnetic radiation, with the representative frequency $\hbar\omega = 1.55$ eV (corresponding to 800 nm wavelength), where we expect the ionic contributions to the elasto-optic response to be negligible, and (2) the THz radiation with $\hbar\omega = 4$ meV (corresponding to 1 THz electromagnetic waves), where we expect that the ionic contributions described in Eq. (5) will be significant, e.g., for p_{3333}^{E}, but far enough from resonances where strong absorption limits the interest of the elasto-optic response. In the latter case, we will, for

the sake of illustration, practically compute the ionic contribution to p^E_{3333} from the finite differences of the static ionic dielectric permittivity obtained from the Monte-Carlo simulations. Note also that, since the central E-mode is soft in our simulations (1 THz or smaller), we expect a large absorption to take place for THz electromagnetic waves polarized in the plane perpendicular to the polarization, which is thus of very limited interest. As a result, we do not investigate the THz elasto-optic response associated with the elasto-optic tensor components p^E_{1111}, p^E_{1122}, p^E_{1212}, p^E_{1313}, and p^E_{1133} which mainly depend on the E-mode. We thus focus only on p^E_{3333} when investigating the elasto-optic response at 1 THz.

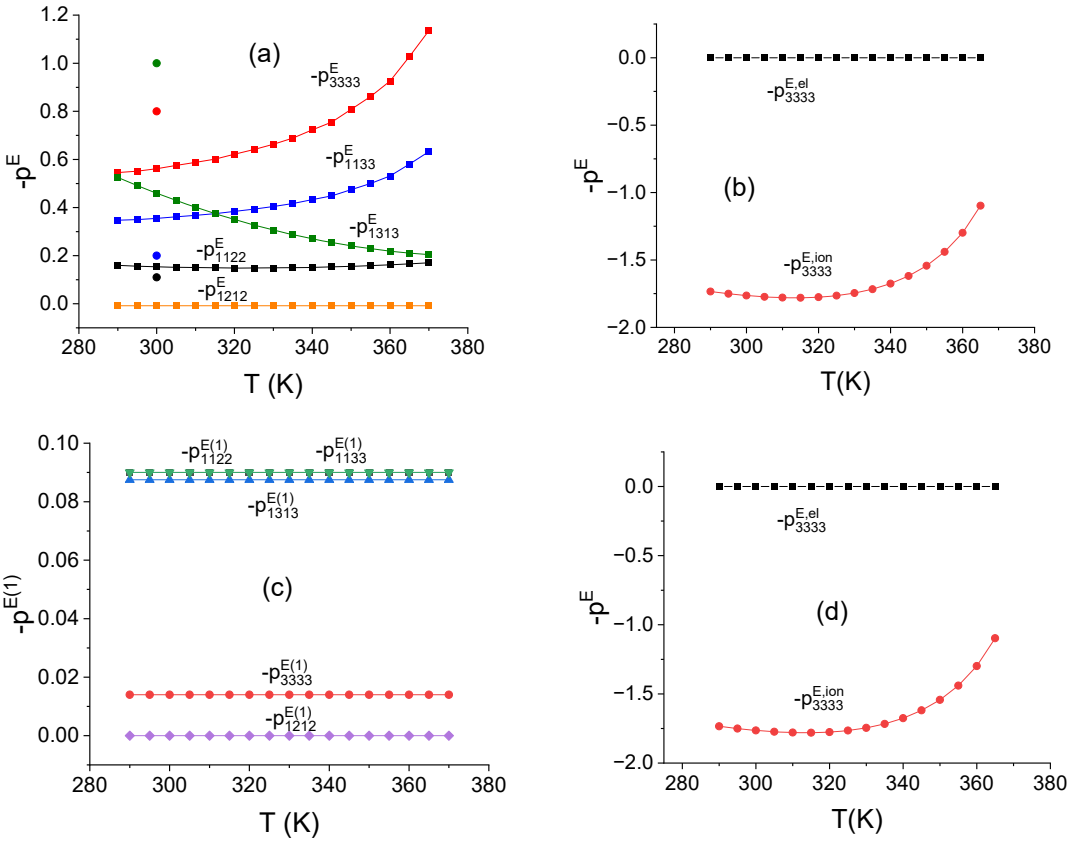


FIG. 1. Temperature dependence of some elasto-optic coefficients in BTO at $\hbar\omega = 1.55$ eV (a) and $\omega = 1$ THz (b); Experimental data [15] are shown in full circles of the same color as the corresponding calculation; The first term in eq. 1 (c); Decomposition of the THz total result for p^E_{3333} into the electronic and ionic parts (d).

We are now able to compute the elasto-optic coefficients at finite temperature. Let us focus on the case of pure tetragonal BTO. Tetragonal BTO appears between 280 and

385 K according to our effective Hamiltonian scheme [22], in reasonable agreement with experimental orthorhombic–to–tetragonal and tetragonal–to–cubic transition temperatures of 278K and 403K, respectively.

Figure 1a shows our computed temperature dependence of the elasto-optic coefficients p^E_{3333}, p^E_{1133}, p^E_{1122}, p^E_{1212}, and p^E_{1313} for ω corresponding to $\hbar\omega = 1.55$ eV (or 800 nm wavelength). Our calculations predict values of 0.56 and 0.36 for $-p^E_{3333}$ and $-p^E_{1133}$ at 300K respectively. They agree reasonably well with the experimental absolute values of 0.8 and 0.2 reported in Ref. [15]. In particular, it is worthwhile to realize that a change of 50K (from 300K to $\simeq$ 350K) gives a computational value of $-p^E_{3333}$ of about 0.8 too. We therefore attribute the quantitative differences largely to the slight underestimation of the tetragonal-to-cubic transition temperature (by about 20 K) in our effective Hamiltonian. On the other hand, our simulations provide a $-p^E_{1313}$ of 0.46 at room temperature, which is half the experimental value of 1.0 [15]. One possibility for this disagreement may be the difficulty of the effective Hamiltonian to model well this coefficient because, e.g., such scheme only incorporates few phonons or rather the possibility that the experiments in fact determined the *sum* of $-p^E_{1313}$ and $-p^E_{1331}$. Novel experiments are thus called for to resolve such issue. Regarding the $-p^E_{1122}$ coefficient , we obtain a value of 0.15 at 300 K, which is rather close to the experimental result of Ref. [15] providing 0.11. On the other hand, we are not aware of any measurement of $-p^E_{1212}$. We thus hope that our prediction of -0.01 at room temperature will be checked soon.

Figure 1a also reveals that both $-p^E_{3333}$ and $-p^E_{1133}$ increase with temperature and are thus maximal at the boundary between the tetragonal and cubic phases, reaching values over 1.14 and 0.63, respectively. In contrast, $-p^E_{1313}$ is a decreasing function of the temperature and therefore adopts its largest value, of around 0.46, near the transition between the orthorhombic and tetragonal ferroelectric phases. This difference stems from the fact that $-p^E_{3333}$ and $-p^E_{1133}$ depend on P_3 and η_{33} (see Eq. (1) of the Supplemental Material [16]), and that the absolute value of the derivative $\frac{dP_3}{d\eta_{33}}$ strongly increases with temperature in the tetragonal phase (one can in fact show that this derivative is inversely proportional to the polarization [29]). In contrast, $-p^E_{1313}$ depends on P_1 and η_{13} [16], and the calculations show that the derivative of P_1 with respect to η_{13} is becoming larger when approaching the tetragonal-to-orthorhombic phase boundary. This explains the increase of p^E_{1313} at this boundary. Note that the elasto-optic responses depicted in Fig. 1 are rather large compared

to other materials, since they even surpass the one of 0.55 found in $BiFeO_3$ [30] and the one of 0.45 magnitude predicted in Ref. [31] for an epitaxial $PbTiO_3$ thin film. Notice also that the temperature dependence of $-p^E_{1122}$ reveals a minimum around 325 K, which is the result of a weak well in the temperature dependence of the absolute value of $\frac{dP_3}{d\eta_{22}}$ (this derivative has negative sign). At last, the coefficient p^E_{1212} does not depend on temperature because it does not involve any derivative of the polarization with respect to the strain owing to the symmetry of the piezoelectric tensor in the $P4mm$ phase [16].

We also numerically found that most of the p^E_{3333} elasto-optic effect at 800 nm comes from the second term in Eq.(4). For example, at 290 K at which $-p^E_{3333} = 0.55$, the first term of Eq.(4) is only 0.01 – which therefore amounts to only 1.8% of the total value. The relative contribution of the temperature-independent first term of Eq.(4) thus further decreases for $-p^E_{3333}$ as the temperature increases. Regarding $-p^E_{1133}$, which is equal to 0.35 at 290K, the first term of Eq.(4) contributes more significantly, since its value of 0.09 represents 25.7% of the total coefficient. Such latter percentage decreases to 14.3% at 370K for which $-p^E_{1133} = 0.63$. As for $-p^E_{1313}$, the first term is 0.09 and the values at 290 and 370K are 0.53 and 0.20 correspondingly – which therefore renders the first term contributing to 17% and a significant 45%, respectively, to the total $-p^E_{1313}$. Finally, the first term in $-p^E_{1122}$ has a temperature-independent value of 0.09, while the total value of this coefficient at these temperatures is 0.16 and 0.17 at 290 and 370K, respectively, resulting in the contribution of the first term by 56% and 53% correspondingly.

For an ω frequency of 1 THz, we find a threefold increase of the magnitude of $-p^E_{3333}$ at 300 K and a sign reversal compared to its value in the visible range discussed above (see Figure 1b). This dramatic magnitude increase is driven, in large part, by the ionic contribution detailed in Eq. (5), which is opposite in sign to the electronic contributions reported in Eq. (4). In fact, in the THz regime, and at 300 K, the electronic contribution to $-p^E_{3333}$ of the computations of the elastooptic coefficients provided by Eq. (4) is only 0.2% of its total value: the electronic contributions to $-p^E_{3333}$ amount to -0.004, whereas the total value is -1.76. This happens for two main reasons: (1) the dielectric permittivity in the denominator of Eq. (4) includes now not only the electronic but also the ionic part, which, in ferroelectric BTO, is rather significant; and (2) $\frac{d\chi^{ion}_{ij}(\nu)}{d\eta_{\alpha\beta}}$ is very large in magnitude in Eq. (5), which therefore makes $-p^E_{3333}$ large in strength. Note also that this latter derivative is negative, reflecting the fact that increasing the η_{33} strain enhances the z-component of the

polarization and this decreases the dielectric ionic susceptibility χ_{33}. Consequently, $-p^E_{3333}$ is now negative, in contrast with the optical frequencies results. Varying the frequency ω in ferroelectric BTO therefore can induce not only an enhancement of the magnitude of the elasto-optic response but also a change of its sign. Similarly, the temperature dependence of the $-p^E_{3333}$ elasto-optic coefficient is markedly different for frequencies ω in the THz (Fig. 1b) compared to the visible frequencies (Fig. 1a). Indeed, for $\omega = 1$ THz, $-p^E_{3333}$ is largest in magnitude and fairly constant at temperatures close to the tetragonal-to-orthorombic phase transition, while its magnitude is strongly reduced near the tetragonal-to-cubic phase transition temperature (see Fig. 1b).

Let us now investigate the composition dependence of $-p^E_{3333}$, $-p^E_{1133}$ and $-p^E_{1313}$ in $(Ba_{1-x}Sr_x)TiO_3$ solid solutions, at a room temperature of 300K, which are depicted in Fig. 2a for ω corresponding to a visible wavelength of 800 nm. In the visible range, $-p^E_{3333}$ and $-p^E_{1133}$ both increase with the Sr composition, x, until $x = 0.24$, corresponding to the boundary between the tetragonal and cubic phases. In contrast, $-p^E_{1313}$ is reduced when the Sr concentration increases. Indeed, $-p^E_{1313}$ is maximum at $x = 0$, where, as this is seen from Fig. 1a, BTO is close to the tetragonal-to-orthorhombic phase boundary. Our calculations show that the reason for this qualitatively different compositional behavior of $-p^E_{3333}$ and $-p^E_{1133}$ from the one hand, and $-p^E_{1313}$ from the other stems from the increase with x of the absolute value of the derivative $\frac{dP_3}{d\eta_{33}}$ and from the decrease of $\frac{dP_1}{d\eta_{13}}$: the former defines $-p^E_{3333}$ and $-p^E_{1133}$ while the latter is associated with $-p^E_{1313}$, as demonstrated by Eq.(1) of the Supplemental Material [16]. Note also that the first term in Eq. (4) is typically negligible in comparison with its second term. Indeed, in BTO at 300 K and for ω in the visible range, the first term in Eq. (4) contributes 0.01 to $-p^E_{3333}$ (for a total value of 0.56), 0.09 to $-p^E_{1133}$ (0.35 total value) and 0.09 to $-p^E_{1313}$ (0.46 total value). The maximum relative contribution of the first term in Eq. (4) occurs at $x \approx 0.24$ for the coefficient $-p^E_{1313}$. Indeed, at $x = 0.24$, we have 0.07 for the first term of $-p^E_{1313}$ to be compared with the total value of 0,24 (we also have 0.01 for p^E_{3333} (1.15 total value) and 0.09 for $-p^E_{1133}$ (0.59 total)).

Figure 2b shows our calculated $-p^E_{3333}$ at 1 THz frequency. Similarly to BTO, the elasto-optic coefficients $-p^E_{3333}$ is negative for $\omega = 1$ THz, for all studied concentrations x. As in BTO, this is mainly due to (1) the large amplitude of the ionic contribution of Eq. (5) and (2) the large dielectric permittivity at 1 THz (due to a strong ionic contribution) in the denominator of Eq. (4). As already observed with temperature in the case of BTO

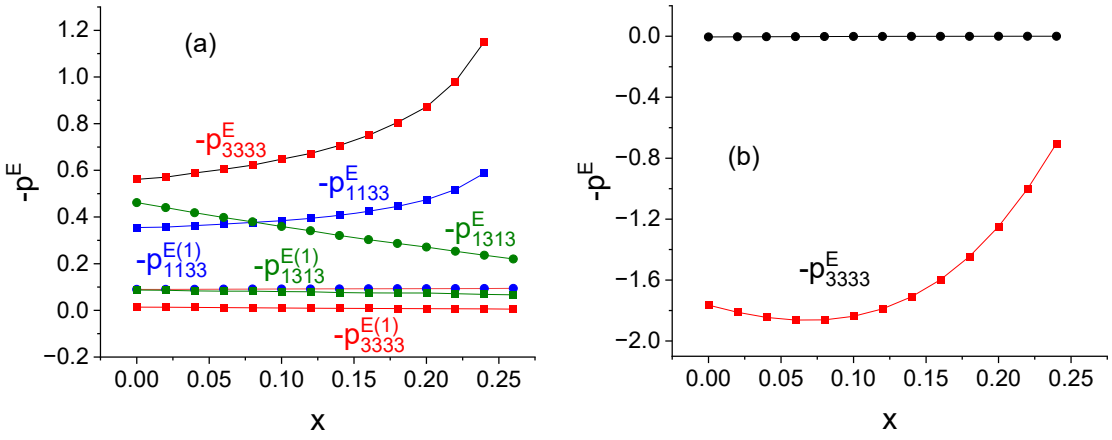


FIG. 2. Concentration dependence of some elasto-optic coefficients in BST at room temperature at $\hbar\omega = 1.55$ eV (a) and $\omega = 1$ THz (b). Slide (a) also shows the contribution to the total result of the first term in eq. 4.

(see Fig. 1b), we similarly notice that the amplitude of $-p^E_{3333}$ is strongly reduced when approaching $x = 0.24$. Such decrease is caused by the strong increase of the ionic dielectric permittivity, due to the proximity to the tetragonal-to-cubic phase boundary, and which is involved in the denominator of Eq. (5).

In conclusion, we developed a calculation scheme to predict the linear elasto-optic response of materials by coupling DFT and effective Hamiltonian-based simulations. Applying this method to the case of $Ba_{1-x}Sr_xTiO_3$ and $BaTiO_3$, we show that the composition- or temperature-driven phase transitions significantly improve some elasto-optic coefficients. We reveal that the ionic contributions dominate the elasto-optic response in the THz regime due to the effect of the optical phonons in this regime on the refraction coefficient, while the electronic contributions are the main component of the elasto-optic response in the visible

part of the electromagnetic spectrum. This novel method of calculating the elasto-optic response opens new ways to search and engineer materials with high-performance elasto-optic responses at room temperature.

ACKNOWLEDGMENTS

The authors thank the support of Grant number FA9550-23-1-0500 from ONR (Depscor), Grant number PA-23-01-03-ATOM-FP-004 from DARPA and the Vannevar Bush Faculty Fellowship (VBFF) Grant No. N00014-20-1-2834 from the Department of Defense. C. P. acknowledges partial support from Agence Nationale de la Recherche (ANR) under Grant no. 21-CE42-0030 (THz-MUFINS).

---

[1] N. Mohammad, W. Szyszkowski, W. J. Zhang, E. I. Haddad, J. Zou, W. Jamroz, and R. Kruzelecky, Analysis and Development of a Tunable Fiber Bragg Grating Filter Based on Axial Tension/Compression, Journal of Lightwave Technology **22**, 2001 (2004).

[2] L. Cai, A. Mahmoud, M. Khan, M. Mahmoud, T. Mukherjee, J. Bain, and G. Piazza, Acousto-optical modulation of thin film lithium niobate waveguide devices, Photonics Research **7**, 1003 (2019).

[3] B. Nelson, Optical differential strain gauge, US Patent 4777358 (1988).

[4] M. Veithen, X. Gonze, and P. Ghosez, Nonlinear optical susceptibilities, Raman efficiencies, and electro-optic tensors from first-principles density functional perturbation theory, Phys. Rev. B **71**, 125107 (2005).

[5] M. Veithen, X. Gonze, and P. Ghosez, First-Principles Study of the Electro-Optic Effect in Ferroelectric Oxides, Phys. Rev. Lett. **93**, 187401 (2004).

[6] A. Mahmoud, A. Erba, Kh. E. El-Kelany, M. Rérat and R. Orlando, Low-temperature phase of $BaTiO_3$: Piezoelectric, dielectric, elastic, and photoelastic properties from ab initio simulations, Phys. Rev. B **89**, 045103 (2014).

[7] S. H. Wemple and M. DiDomeniko, Theory of the Elasto-Optic Effect in Nonmetallic Crystals, Phys. Rev. B **1**, 193 (1970).

[8] M. G. Cohen, M. DiDomenico, Jr. , and S. H. Wemple, Influence of Critical Polarization

Fluctuations on the Photoelastic Behavior of $BaTiO_3$, Phys. Rev. B, **1**, 4334 (1970).

[9] S. Prosandeev, C. Paillard, and L. Bellaiche, Crossover from Linear to Quadratic Electro-optic Behavior in $BaTiO_3$ and (Ba,Sr)TiO_3 Solid Solution, Phys. Rev. Lett. **132**, 196901 (2024).

[10] A. Erba and R. Dovesi, Photoelasticity of crystals from theoretical simulations, Phys. Rev. B **88**, 045121 (2013).

[11] C. Paillard, S. Prokhorenko, and L. Bellaiche, Strain engineering of electro-optic constants in ferroelectric materials, npj Comput. Mater. **5**, 6 (2019).

[12] Z. Jiang, C. Paillard, D. Vanderbilt, H. Xiang, and L. Bellaiche, Designing Multifunctionality via Assembling Dissimilar Materials: Epitaxial AlN/ScN Superlattices, Phys. Rev. Lett. **123**, 096801 (2019).

[13] F. Delodovici, C. Atkinson, R. Xu, P.-E. Janolin, S. P. Alpay, C. Paillard, Engineering the electro-optic effect in HfO_2 and ZrO_2 through strain and polarization control, J. Appl. Phys. **134**, 055108 (2023).

[14] M. Veithen and Ph. Ghosez, Temperature dependence of the electro-optic tensor and refractive indices of $BaTiO_3$ from first principles, Phys. Rev. B **71**, 132101 (2005).

[15] M. Zgonik, P. Bernasconi, M. Duelli, R. Schlesser, P. Gunter, M. H. Garrett, D. Rytz, Y. Zhu, and X. Wu, Dielectric, elastic, piezoelectric, electro-optic, and elasto-optic tensors of $BaTiO_3$ crystals, Phys. Rev. B **50**, 5941 (1994).

[16] See Supplemental Material at [URL will be inserted by publisher] for the explicit expression of the elasto-optic coefficients in the $P4mm$ phase of BTO and BST, in relation to the piezoelectric tensor [19], technical details on the numerical calculations of derivatives of the electronic dielectric constant with respect to polarization and strains, involving Berry-phase calculations [20, 21], as well as technical details on the finite temperature derivatives of the polarization with respect to the strain calculated within the effective Hamiltonian scheme [22].

[17] W. Zhong, D. Vanderbilt, and K. M. Rabe, Phase Transitions in $BaTiO_3$ from First Principles, Phys. Rev. Lett. **73**, 1861 (1994).

[18] W. Zhong, D. Vanderbilt, and K. M. Rabe, First-principles theory of ferroelectric phase transitions for perovskites: The case of $BaTiO_3$, Phys. Rev. B **52**, 6301 (1995).

[19] L. Bellaiche, A. Garcia, and D. Vanderbilt, Low-Temperature Properties of $Pb(Zr_{1-x}Ti_x)O_3$ Solid Solutions near the Morphotropic Phase Boundary, Ferroelectrics **266**, 41 (2002).

[20] R. Resta, Manifestations of Berry's phase in molecules and in condensed matter. J. Phys.:

Condens. Matter. **12**, R107 (2000).

[21] D. Vanderbilt, Berry Phases in Electronic Structure Theory: Electric Polarization, Orbital Magnetization and Topological Insulators. Cambridge University Press, Cambridge. (2018). https://doi.org/10.1017/9781316662205.

[22] L. Walizer, S. Lisenkov, and L. Bellaiche, Finite-temperature properties of (Ba,Sr)TiO_3 systems from atomistic simulations, Phys. Rev. B **73**, 144105 (2006).

[23] X. Gonze, J.-M. Beuken, R. Caracas, F. Detraux, M. Fuchs, G.-M. Rignanese, L. Sindic, M. Verstraete, G. Zerah, F. Jollet, M. Torrent, A. Roy, M. Mikami, P. Ghosez, J.-Y. Raty, and D. C. Allan, First-principles computation of material properties: the ABINIT software project, Comput. Mater. Sci. **25**, 478 (2002).

[24] D. R. Hamann, Optimized norm-conserving Vanderbilt pseudopotentials, Phys. Rev. B **88**, 085117 (2013).

[25] L. Bellaiche and D. Vanderbilt, Virtual crystal approximation revisited: Application to dielectric and piezoelectric properties of perovskites, Phys. Rev. B **61**, 7877 (2000).

[26] J. L. P. Hughes and J. E. Sipe, Calculation of second-order optical response in semiconductors, Phys. Rev. B **53**, 10751 (1996).

[27] E. K. H. Salje, M. A. Carpenter, G. F. Nataf, G. Picht, K. Webber, J. Weerasinghe, S. Lisenkov, and L. Bellaiche, Elastic excitations in $BaTiO_3$ single crystals and ceramics: Mobile domain boundaries and polar nanoregions observed by resonant ultrasonic spectroscopy, Phys. Rev. B **87**, 014106 (2013).

[28] J. Hlinka, T. Ostapchuk, D. Nuzhnyy, J. Petzelt, P. Kuzel, C. Kadlec, P. Vanek, I. Ponomareva, and L. Bellaiche, Coexistence of the Phonon and Relaxation Soft Modes in the Terahertz Dielectric Response of Tetragonal $BaTiO_3$, Phys. Rev. Lett. **101**, 167402 (2008).

[29] A. K. Tagantsev, L. E. Cross, J. Fousek, Domains in Ferroic Crystals and Thin Films (Springer, New York 2010).

[30] D. Sando, Y. Yang, E. Bousquet, C. Carrétéro1, V. Garcia, S. Fusil, D. Dolfi, A. Barthélémy, Ph. Ghosez, L. Bellaiche, and M. Bibes, Large elasto-optic effect and reversible electrochromism in multiferroic $BiFeO_3$, Nature Communications **7**, 10718 (2016).

[31] L. Chen, Y. Yang, Z. Gui, D. Sando, M. Bibes, X. K. Meng, and L. Bellaiche, Large Elasto-Optic Effect in Epitaxial $PbTiO_3$ Films, Phys. Rev. Lett. **115**, 267602 (2015).